Multi-objective Optimization of Turning Ti-6Al-4V Titanium Alloy Using Design of Experiments, Artificial Neural Networks and Genetic Algorithms

Anas Chtioui
LCPMA Laboratory, FS Ben M'sik
Hassan II university, Driss El Harti St.
Casablanca
Morocco

Aissa Ouballouch
C3S Laboratory, ESTC, Hassan II
university, Road El Jadida Km 7, Oasis
Casablanca
Morocco

Ahmed Mouchtachi
LCPMA Laboratory, FS Ben M'sik
Hassan II university, Driss El Harti St.
Casablanca
Morocco

This paper presents an experimental investigation into the machinability of Ti-6Al-4V titanium alloy. It focuses on the influence of cutting parameters on quality and productivity of machined parts. A Taguchi L27 orthogonal array combined with analysis of variance is used to evaluate the significance of machining parameters and their interactions. Multi-objective optimization based on desirability function (DF) is performed to determine the optimal cutting parameters. Moreover, a hybrid artificial neural networks–genetic algorithms (ANN-GA) model based on Taguchi L27 and coupled to DF is adopted to predict and optimize cutting responses. ANN-GA-DF exhibits superior performance, achieving significant improvements in surface roughness (39% in Ra, 19% in Rq, 24% in Rz), dimensional and geometric accuracy (25% and 39%, respectively). Material removal rate decines slightly (5.3%). Optimal parameters are tool radius of 0.4mm, cutting speed of 25 m/min, feed rate of 0.065 mm/rev, and depth of cut of 0.7 mm.

Keywords: *Turning; Ti-6Al-4V; multi-objective optimisation; artificial neural networks; genetic algorithms.*

1. INTRODUCTION

Ti-6Al-4V titanium alloy is extensively used in advanced technology sectors, including aeronautics, naval ships, nuclear, and biomedical applications, due to its combination of strength, light weight, outstanding corrosion resistance, and biocompatibility [1–3]. However, machining Ti-6Al-4V presents significant challenges and remains a costly process [4,5]. Titanium alloys have low thermal conductivity, high heat capacity, high rigidity, high chemical reactivity at elevated temperature, and diffusivity, along with low elastic modulus. These properties promote heat accumulation and strong adhesion in the cutting zone [6,7], leading to accelerated tool wear and degraded surface integrity [8–10]. Consequently, Ti-6Al-4V is regarded as a difficult-to-cut material, exhibiting serrated chip formation [11,12], pronounced cutting force fluctuations, and a significant vibrations that affect the process stability [13–17]. Therefore the quality of machined parts is adversely affected, resulting in limitation in surface roughness, dimensional accuracy and geometric tolerances [18,19], which are critical for components with stringent functional requirements. Optimizing cutting parameters is a key factor in achieving superior quality and process productivity. Stringent quality requirements for machined parts are often prioritised, while production costs are considered of secondary importance. The quality of machined parts is primarily governed by the surface roughness, characterized by the arithmetic mean roughness (Ra), the root mean square roughness (Rq), and the maximum peak-to-valley height (Rz), as well as by their dimensional and geometric accuracy. A specified target surface roughness is often essential to ensure the required fatigue performance [20,21]. However, achieving superior surface finish and tighter tolerances often conflict with productivity and cost-effectiveness. As a result, it's important to establish an optimum balance between the quality of finished parts and theirs process productivity. Many researches highlighted the high sensitivity of machining responses to a multitude of interdependent factors. These include the tool-workpiece system, encompassing material properties and geometries, as well as process parameters such as cutting speed, feed rate, depth of cut, and lubrication conditions [22–32].

Numerous studies have addressed the optimization of cutting process using statistical approaches such as analysis of variance (ANOVA), regression modelling, and response surface methodology (RSM) within the framework of Design of Experiments (DoE). Yan et al. [33] performed a multi-objective optimization study on the effects of milling parameters on surface roughness, material removal rate (MRR), and cutting energy consumption, using a weighted grey relational analysis combined with RSM. Their results identified the width of cut as the most significant parameter, while lower spindle improved energy efficiency. Ramesh et al. [34] investigated the optimization of turning Ti-6Al-4V by minimising surface roughness, varying cutting speed (80–280 m/min), feed rate (0.06–0.21 mm/rev), and depth of cut (0.5–1 mm). Based on DoE and RSM the feed rate is identified as the most influential parameter.

Received: May 2026, Accepted: June 2026
Correspondence to: Anas Chtioui
LCPMA Laboratory, FS Ben M'sik Hassan II University, Driss El Harti St. Casablanca, Morocco
E-mail: anas.chtioui@gmail.com
doi:10.5937/fme2603498C

Rahman et al. [35] carried out a multi-objective optimization of Ti-6Al-4V face milling using Taguchi design, ANOVA, and grey relational analysis. The results shows that the radial depth of cut was the most influential parameter. Cica et al. [36] conducted an investigation to improve surface integrity, reduce energy consumption, and enhance productivity during Ti-6Al-4V milling. The ANOVA results highlighted the significant effect of feed per tooth, cooling strategy, and cutting speed on the responses. Jamil et al. [37] focused on energy consumption, surface roughness, tool wear, and chip formation. Using ANOVA, regression analysis and DF. The result revealed that cutting speed mainly governs energy consumption, while feed per tooth dominates surface quality. Aggressive machining parameters were reported to increase tool wear and promote serrated chips. Khan et al. [38] conducted a multi-objective study on Ti-6Al-4V turning considering feed rate, cutting speed, depth of cut, and cutting environment (dry, flooded and cryogenic), in terms of cutting energy, tool wear, surface roughness and material removal rate. Using Taguchi, grey relation, ANOVA, regression, and RSM. They identified feed rate as the dominant parameter affecting overall perfor–mance. Kumar et al. [39] investigated the effect of cut–ting speed, feed rate, axial depth of cut and concen–tration of eco-friendly multi-walled carbon nanotube on cutting force, cutting temperature and MRR. The developed lubrication system improved performance across all measured response. Younas et al. [40] studied the optimal combination of turning parameters for Ti-6Al-4V, considering tool wear, surface, and material removal rate. Their results showed a significant inte–raction effect between feed rate and cutting speed. Hossain et al. [41] analysed the effect of cutting conditions on surface finish of Ti-6Al-4V and tool-chip interface temperature, using RSM and ANOVA to determine optimal cutting conditions. Hence, there is a strong need to explore hybrid intelligent approaches and their potential for optimization and prediction.

Recent trends in the increase of the use of artificial intelligence (AI) methods in manufacturing processes, have created new opportunities for process optimisation and robust performance prediction, supported by recent technological advances. Artificial neural networks (ANN) are now widely used to model highly nonlinear interaction between process parameters and their responses. In machining, numerous studies have shown that ANN trained on experimental data can predict key performance indicators with high accuracy [42–45]. Increasing attention has been directed toward metaheuristic methods and hybrid ANN–GA strategies [46–49]. Several researches have demonstrated the effectiveness of ANN-based models. Li et al. [50] used ANN coupled with Non-Dominated Sorting Genetic Algorithm II (NSGA-II) to optimise Ti-6Al-4V milling, leading to simultaneous improvements in production costs, surface quality and residual stress. Indira et al. [51] performed a multi-objective optimization of Ti-6Al-4V finish milling, using ANN–based modelling and particle swarm optimization (PSO) to minimize cutting temperature and surface roughness. Mane et al. [52] carried out a predictive model for surface roughness and cutting temperature in hard turning of AISI 52100 steel under Minimum Quantity Lubrication conditions using RSM and ANN. The ANN model shows higher predictive accuracy for both responses compared to quadratic RSM model. Elsadek et al. [53] studied the effects of cutting speed, feed rate, depth of cut, and workpiece hardness on the temperature generated at the tool/workpiece interface when hard turning AISI H13 steel. They applied RSM and ANN for predictive, and cuttlefish algorithm (CFA) and GA to optimize the cutting responses. Mia et al. [54] performed a multi-objective optimisation of Ti-6Al-4V cryogenic turning, focusing on surface roughness, and cutting forces, using a Taguchi L18, RSM and ANN, coupled to DF.

The literature reveals that most optimization studies on Ti-6Al-4V turning have mainly considered surface roughness as the dominant quality response, whereas dimensional and geometric accuracy are also critical criteria for functional performance. Moreover, productivity is often treated as a secondary objective, although it directly affects machining efficiency. Consequently, responses may lead to conflicting optimal cutting conditions. In this context, intelligent manufacturing based on AI tools, even with limited experimental data, represents a promising solution for addressing multi-objective optimization challenges. Accordingly, the current study puts forward a comprehensive hybrid approach, integrating and comparing classical statistical tools with advanced AI techniques. It aims to identify cutting conditions that provide a balanced trade-off between product quality and machining productivity. The major contribution of this work is to demonstrate the effectiveness of a hybrid approach. This approach operates within a global multi-objective optimization framework. It particularly applied to the turning of Ti-6Al-4V titanium alloy. This material is commonly considered as a difficult-to-cut material, and widely used in critical components, especially in the aeronautical sector. Using DoE, ANOVA, ANN and GA, this study proposes a multi-objective optimisation strategy for Ti-6Al-4V turning. Initially, the effects of the main cutting parameters (tool nose radius, cutting speed, feed rate, and depth of cut) on the key responses are quantified. The considered responses include part quality (surface roughness characterized by Ra, Rq, and Rz), dimensional and geometric accuracy, as well as productivity measured by MRR. A composite DF is used to determine an optimal trade-off among machining responses. A hybrid ANN-GA strategy is implemented, ANN models provide an accurate estimation of responses, while GA allows for simultaneous, guided, multi-objective searching in the parameter space. This paper is structured as follows: the material and methods are presented first, followed by the analysis and discussion of the experimental results, and Finally a conclusion summarizes the main findings.

2. MATERIAL AND METHODS

This section describes: material, experimental set-up, and testing procedure.

2.1 Work material and machine tools

The material investigated in this study is a biphasic (α + β) titanium alloy, Ti-6Al-4V. Its standardized chemical composition and mechanical properties are listed in Table 1 and Table 2 respectively. The material was supplied in the form of solid cylindrical bars with a diameter of 14 mm and a length of 1 m. The work material consists of standardized cylindrical specimens, manufactured according to ASTM E466 specifications. The specimen geometry and dimensions are presented in Figure 1. The specimens were machined on a JHFTMT MJ-50 CNC lathe (Figure 2). This machine had a spindle power of 26 kW and a maximum speed of 3500 rpm. The cutting parameters and their range are tabulated in Table 3. The factor levels were ascertained based on preliminary bounding tests, the specifications and the recommendations of the tool manufacturer, and industrial expertise. To eliminate the influence of tool wear, a new insert was used for each trial during the finishing operation, which was performed in a single pass. Similarly, the fixed parameters were kept constant for the entire experimental design. The cutting inserts used in this study are CVD TiAlN-coated carbide inserts from Sandvik CoroTurn 107. The inserts are mounted and fixed by a screw on a tool holder of type SDNCN2525M11. The geometry of insert and tool holder are is illustrated in Figure 3a et 3b respectively.

The specimens were machined according to the required dimensions specified in drawing Figure 1a. To guarantee the reproducibility of the measurements, the experiments were repeated three times, using a new insert for each trial. The optimal ranges of cutting conditions were selected based on industrial and tool manufacturer guidelines, and subsequently validated experimentally. This selection also accounted for the performance limits and operating capabilities of the machine tool. To limit heat generation at the tool-workpiece interface and to facilitate chip evacuation, lubricated machining was adopted. The lubrication mode was provided using a water-soluble cutting fluid (VASCOMET 10), applied under conventional flood cooling conditions. Typically, flow rate of over 100 L/h is adopted. The application of cutting fluids is performed by directing the nozzle towards the rear of the chip, the rake face, and the flank face.

Table 1. Chemical composition of Ti-6Al-4V

Alloy	Al	V	Fe	C	Ti
Composition %	6.40	0.1	0.16	0.002	93.338

Table 2. Mechanical properties of Ti-6Al-4V

Yield Tensile Strength (MPa)	880
Ultimate Tensile Strength (MPa)	950
Elongation at Break	14 %
Modulus of Elasticity (GPa)	113.8
Poisson’s Ratio	0.342
Density (g/cm3)	4.43

Table 3. Cutting parameters

Parameters	Unit	Symbol	Level 1	Level 2	Level 3
Cutting speed	m/min	*Vc*	17	32	47
Feed rate	mm/rev	*F*	0.05	0.1	0.15
Depth of cut	mm	*Af*	0.25	0.5	0.75
Tool radius	mm	*Rbec*	0.2	0.4	0.8

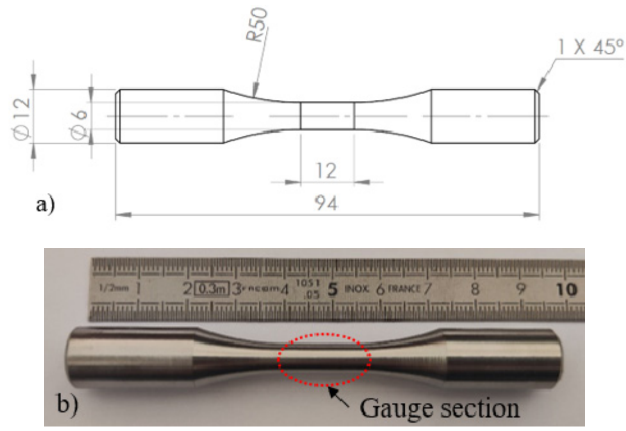

Figure 1. Specimen, a) 2D drawing, b) Machined part

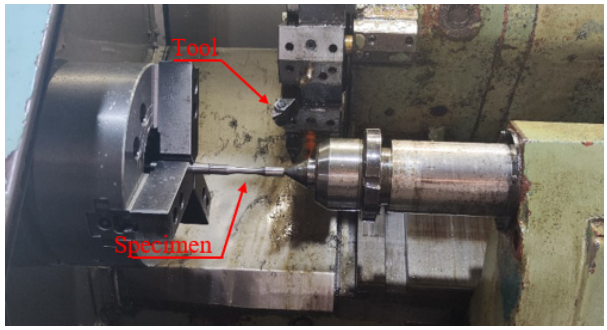

Figure 2. CNC lathe machine setup for experimentation

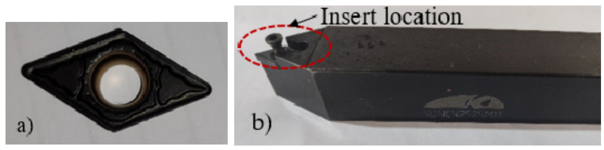

Figure 3. a) Insert, b) Cutting tool holder

2.2 Work material and machine tools

The output responses considered in this study are the three surface roughness parameters (Ra, Rq and Rz), dimensional and geometric deviation, and material removal rate. The surface parameters are measured using a Mitutoyo SJ-310 tester according to ISO 1997 (Figure 4). The measurements were performed on the effective gauge section of the specimen, corresponding to a cylindrical zone with a diameter of 6 mm and a length of 12 mm. The results were extracted as values for each parameter and a profile graph (Figure 5). Each measurement is an average of 3 independent readings taken in parallel to the specimen axis at different locations on the same specimen. As depicted in Figure 6. The machined surface texture was examined using an Eclipse LV150N optical microscope from Nikon to characterize the geometrical state of the machined surface. The geometric deviation, which is the circularity error associated with the same diameter (6 mm), was evaluated by means of a dial indicator according to the experimental setup illustrated in Figure 7. Dimensional deviation is defined as the deviation of the measured specimen gauge section diameter with respect to the nominal diameter, which is 6 mm. It is obtained by using a Vernier calliper and a micrometer with a resolution of 0.01 and 0.001 mm, respectively.

Figure 4. Surface roughness tester, a) Display unit, b) Detector unit

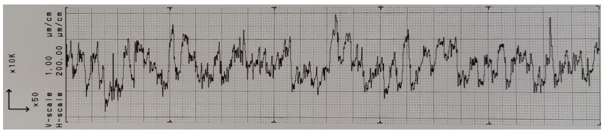

Figure 5. Surface roughness profile under *Vc* 17m/min, *F* 0.05 mm/rev, *Af* 0.5 mm and *Rbec* 0.4 mm

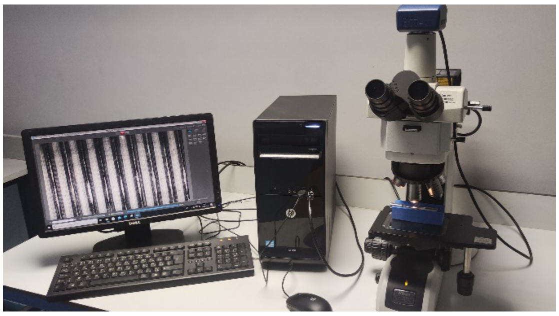

Figure 6. Surface texture analysis under optical microscopy

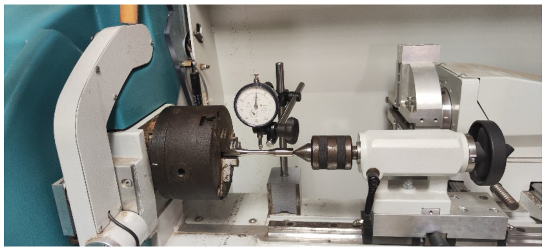

Figure 7. Experimental set-up for geometric specifications control

3. RESULTS AND DISCUSSION

The results section is structured into five sub-sections covering experimental results and Taguchi method, ANOVA, desirability-based optimization, ANN predic–tion, and GA optimization.

3.1 Experimental Results and Taguchi design

Table 4 present the Taguchi L27 orthogonal array used in this study. Experimental design and regression analysis were performed using Minitab 19 software.

The signal-to-noise (S/N) ratios was used to evaluate process variability and noise effects. A smaller-is-better criterion (Equation 1) was applied to Ra, Rq, and Rz, and dimensional and geometric deviation, while a larger-is-better criterion (Equation 2) was adopted for MRR.

$$SN = -10\log_{10}\left(\frac{1}{n}\sum_{i=1}^{n} y_i^2\right) \tag{1}$$

$$SN = -10\log_{10}\left(\frac{1}{n}\sum_{i=1}^{n}\left(y-\bar{y}\right)^2\right) \tag{2}$$

where $\boldsymbol{y_i}$ is the response value at the i[th] repetition, n is the number of repetitions for each response, and □ is the mean of repeated experiments. The ranking of parameter influence on each response is presented in the Table 5.

Table 4. Taguchi L27 orthogonal array design of input parameters and responses

Run N°	Input parameters				Responses					
	Rbec	Vc	F	Af	Ra (µm)	Rq (µm)	Rz (µm)	Dimensional deviation (µm)	Geometric deviation (µm)	MRR (cm3/min)
1	0.2	17	0.05	0.25	1.821	2.215	9.130	6	5	0.519
2	0.2	17	0.1	0.5	2.036	2.256	8.030	8	8	1.024
3	0.2	17	0.15	0.75	3.884	4.615	17.137	12	10	1.515
4	0.2	32	0.05	0.5	1.002	1.238	5.843	6	6	0.964
5	0.2	32	0.1	0.75	2.094	2.545	10.566	8	9	1.902
6	0.2	32	0.15	0.25	3.639	3.005	11.951	8	10	2.932
7	0.2	47	0.05	0.75	1.368	1.683	7.524	12	8	1.397
8	0.2	47	0.1	0.25	1.298	1.544	7.716	10	7	2.871
9	0.2	47	0.15	0.5	3.820	4.626	18.596	12	15	4.248
10	0.4	47	0.05	0.25	1.321	1.613	7.423	10	7	1.436
11	0.4	47	0.1	0.5	1.370	1.656	7.183	12	6	2.832
12	0.4	47	0.15	0.75	1.990	2.416	10.003	14	10	4.190
13	0.4	17	0.05	0.5	0.479	0.787	3.633	8	6	0.512
14	0.4	17	0.1	0.75	1.005	1.190	4.977	8	8	1.010
15	0.4	17	0.15	0.25	1.944	2.253	8.739	9	10	1.558
16	0.4	32	0.05	0.75	0.835	1.017	4.737	8	7	0.951
17	0.4	32	0.1	0.25	1.116	1.358	5.971	6	6	1.955
18	0.4	32	0.15	0.5	1.843	2.169	8.399	8	7	2.892
19	0.8	32	0.05	0.25	0.723	0.894	4.454	10	12	0.977

20	0.8	32	0.1	0.5	0.876	1.072	5.087	8	10	1.928
21	0.8	32	0.15	0.75	1.381	1.680	6.916	9	14	2.853
22	0.8	47	0.05	0.5	0.883	1.094	5.594	10	9	1.416
23	0.8	47	0.1	0.75	1.397	1.702	7.394	15	10	2.793
24	0.8	47	0.15	0.25	1.746	2.087	8.417	16	15	4.307
25	0.8	17	0.05	0.75	0.537	0.665	2.982	9	10	0.505
26	0.8	17	0.1	0.25	0.799	1.002	5.012	10	15	1.039
27	0.8	17	0.15	0.5	1.013	1.202	4.864	10	12	1.536

It can be clearly observed that feed rate and tool nose radius are identified as the most influencing parameters affecting surface roughness and geometric deviation, in agreements with previous studies [55–57]. The increase in Ra with feed rate is mainly attributed to the formation of more pronounced surface peaks and ridges. A small tool nose radius increases vibrations sensitivity, leading to poorer surface quality. Conversely, a larger radius improves surface finish by reducing geometric roughness, but beyond an optimal value it increases cutting forces and vibrations, which deteriorate surface quality. The present findings are in agreement with those reported by Ramesh el al. [34], who investigated Ti6Al4V turning over a range of cutting speeds (80-280 m/min), feed rates (0.06-0.21 mm/rev), and depths of cut (0.5-1 mm). Their results identified feed rate as the most dominant factor affecting surface roughness, while dimensional deviation was mainly influenced by cutting speed, and MRR by both feed rate and cutting speed. Similar findings have been reported by Khan et al.[38], who showed that feed rates and cutting speeds significantly affect MRR in Ti-6Al-4V turning over a range of cutting conditions.

Figure 8 illustrates the evolution of each response parameter in the principal effects plot. Surface roughness decreases with an increase in nose radius, the optimal surface roughness is recorded for a nose radius of 0.8 mm, and increases with an increase of feed rate, the lowest surface roughness is recorded for a feed rate of 0.05 mm/rev. The surface roughness shows a different behaviour with the increase of the depth of cut and cutting speed, it decreases first, then increases.

Table 5. Response table for signal to noise ratios

Smaller is better	Level	Rbec	Vc	F	Af
Ra	1	-6.3831	-1.7038	0.7674	-3.1001
	2	-1.6931	-2.3542	-2.0435	-1.9289
	3	0.1937	-3.8246	-6.6063	-2.8535
	Delta	6.5769	2.1208	7.3738	1.1711
	Rank	2	3	1	4
Rq	1	-7.598	-3.534	-1.307	-4.393
	2	-3.578	-3.687	-3.636	-3.802
	3	-1.554	-5.509	-7.787	-4.535
	Delta	6.044	1.975	6.480	0.732
	Rank	2	3	1	4
Rz	1	-20.00	-15.91	-14.62	-17.30
	2	-16.23	-16.53	-16.49	-16.49
	3	-14.66	-18.45	-19.77	-17.09
	Delta	5.34	2.54	5.15	0.81
	Rank	1	3	2	4
Dim.Dev	1	-18.90	-18.83	-18.66	-19.15
	2	-19.04	-17.84	-19.21	-19.00
	3	-20.43	-21.70	-20.50	-20.22
	Delta	1.53	3.86	1.84	1.22
	Rank	3	1	2	4
Geo.Dev	1	-18.35	-18.97	-17.52	-19.11
	2	-17.27	-18.72	-18.53	-18.43
	3	-21.36	-19.28	-20.94	-19.45
	Delta	4.08	0.56	3.42	1.02
	Rank	1	4	2	3
Larger is better					
MRR	1	4.1514	-0.6243	-1.0363	4.2713
	2	4.1514	4.8697	4.9843	4.1508
	3	4.1514	8.2087	8.5061	4.0320
	Delta	0.0000	8.8330	9.5424	0.2393
	Rank	4	2	1	3

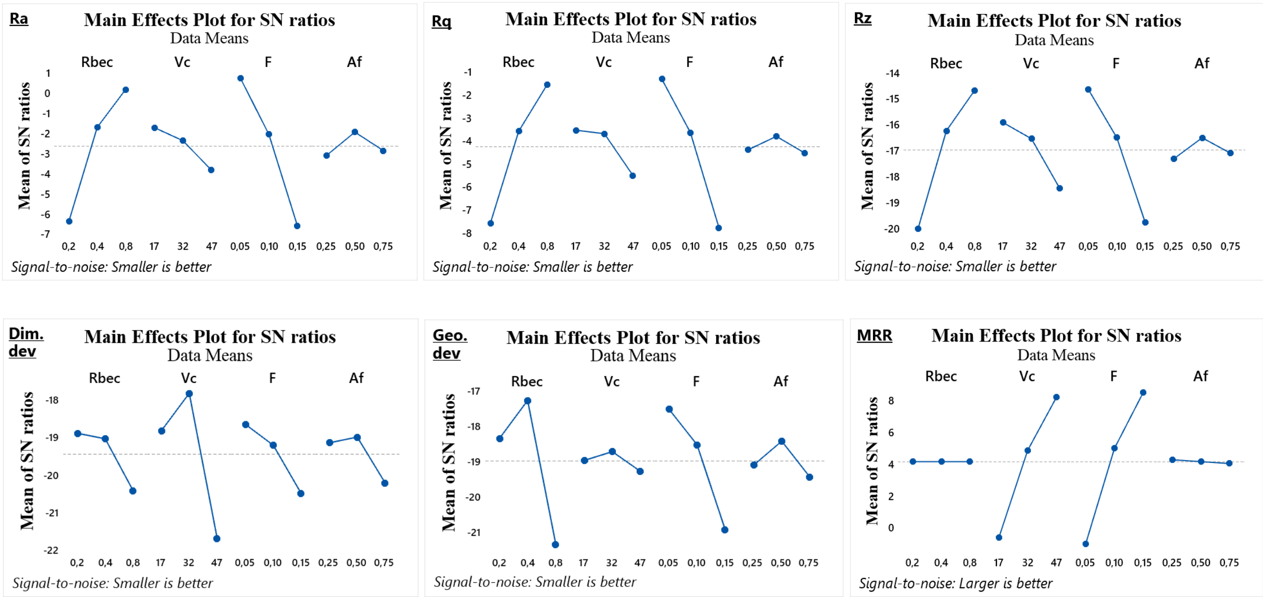

Figure 8. Main effects plot for SN ratios

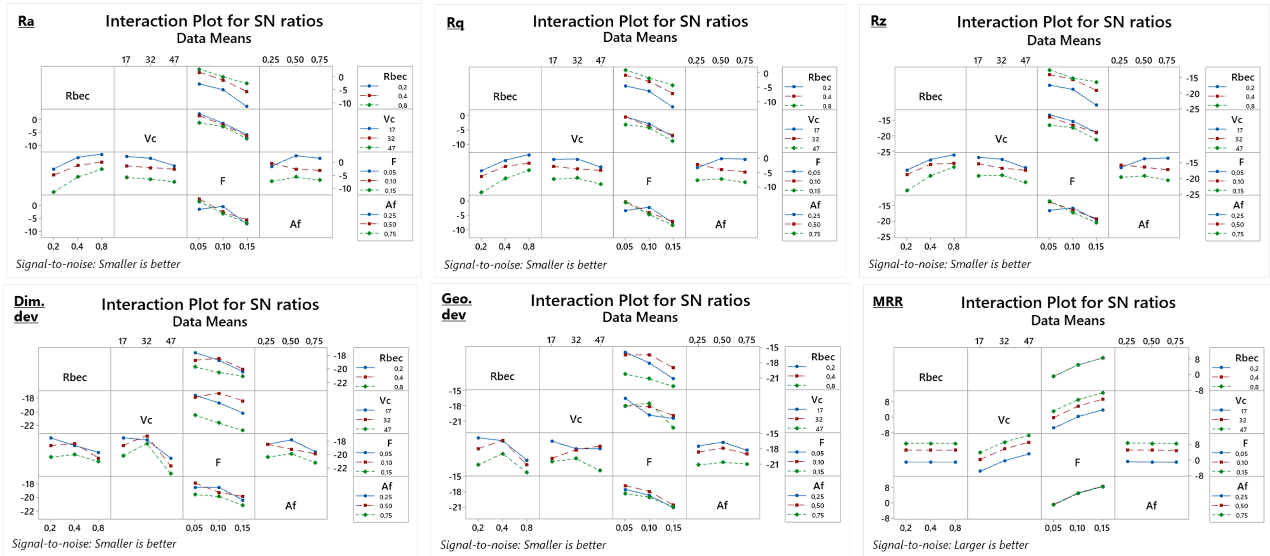

Figure 9. Interaction plots for SN ratios

The best surface roughness is obtained with an average depth of cut of 0.5 mm and a low cutting speed of 17 m/min. Regarding the effect of the process variables on the dimensional deviation, the results shows that this latter decreases with a decrease of tool nose radius and feed rate and decreases first, then increases with increases of cutting speed and depth of cut. The lowest dimensional deviation is obtained with *Rbec* of 0.2, *Vc* of 32 m/min, *Af* of 0.5 mm, and *F* of 0.05 mm/rev. As for the process parameter's effect on the geometrical deviation, this one decreases first, then inc–reases with an increase of depth of cut, tool nose radius, and cutting speed, while it increases with an increase of feed rate. The lowest geometric deviation is achieved with *Rbec* of 0.4 mm, *F* of 0.05 mm/rev, *Vc* of 32 m/min, and a depth of cut of 0.5 mm. Concerning MRR, the pronounced effect of cutting speed and *F* on MRR, it decreases significantly with an increase of cutting speed and feed rate; the lowest geometric deviation is achieved with *Vc* of 47 m/min and a *F* of 0.15 mm/rev.

Based on previous studies and preliminary trials, feed rate was identified as the key parameter for process optimization. Therefore, the analysis was restricted to first-order interactions involving *F* and the other cutting parameters. The considered interactions are *F* × *Vc*, *F* × *Rbec*, and *F* × *Af*. As shown in Figure 9, the interaction plots for responses lack consistent parallelism, making interaction effects difficult to interpret. Consequently, ANOVA is required to quantify interaction contributions.

3.2 Analysis of variance (ANOVA)

ANOVA was conducted to identify the main factors influencing the output responses and to quantify their contribution percentage. P-values less than 0.05 indicate that the corresponding factor has a statistically significant effect on the response, enabling to identify the most influential cutting parameters. The Anderson–Darling normality test was performed at 95% confidence interval. Figure 10 shows a normal distribution of the residuals, satisfying the normality assumption required for ANOVA. The residuals related to Ra, Rq, and Dim.Dev shows a good agreement with the normal probability line, reflecting well-behaved error distributions. Slight deviation is observed at Rz, Geo.Dev, and MRR. However, they remain within the 95% confidence interval, confirming that the normality assumption is met. To verify the random error distribution in the statistical model, residuals-versus-fitted plots for each response were constructed (Figure 11). The graphs shows a random distribution of the residuals around the zero line, confirming that the homoscedasticity assumption is satisfied. No systematic pattern is observed in the residuals, indicating that the assumptions of the independence and constant variance are reasonably satisfied.

ANOVA results (Table 6), quantify the contribution of machining parameters and their interactions. Feed rate identified as the most influential factor affecting surface roughness, contributing 41.10% to Ra, 38.56% to Rq, and 33.64% to Rz. While, *Rbec* exhibits a primary contribution of 37.10% to Rz. For dimensional deviation, cutting speed is the dominant parameter (56.36%), whereas the nose radius contributes 41.99% to geometric deviation. Regarding MRR, cutting speed again has the most significant effect (49.35%), followed by feed rate with a contribution of 43.37%.

Table 6. Analysis of Variance results

Response	Source	DF	Contribution	Adj SS	Adj MS	F value	P value
Ra	Rbec	2	37.29%	8.26961	4.13481	39.40	0.00035
	Vc	2	0.94%	0.20924	0.10462	1.00	0.42282
	F	2	41.10%	9.11348	4.55674	43.43	0.00027
	Af	2	0.43%	0.09438	0.04719	0.45	0.65768
	Vc×F	4	0.43%	0.09610	0.02402	0.23	0.91244
	F×Af	4	3.22%	0.71303	0.17826	1.70	0.26739
	Rbec×F	4	13.75%	3.04971	0.76243	7.27	0.01747
	Error	6	2.84%	0.62959	0.10493		
Rq	Rbec	2	35.40%	9.1602	4.58008	16.78	0.00349
	Vc	2	2.62%	0.6779	0.33897	1.24	0.35383
	F	2	38.56%	9.9788	4.98938	18.27	0.00280
	Af	2	0.63%	0.1626	0.08128	0.30	0.75289
	Vc×F	4	1.93%	0.4991	0.12476	0.46	0.76578
	F×Af	4	4.09%	1.0596	0.26491	0.97	0.48772
	Rbec×F	4	10.44%	2.7023	0.67557	2.47	0.15417
	Error	6	6.33%	1.6381	0.27302		
Rz	Rbec	2	37.31%	128.053	64.0265	20.16	0.00217
	Vc	2	5.28%	18.128	9.0642	2.85	0.13461
	F	2	33.64%	115.446	57.7232	18.17	0.00284
	Af	2	0.42%	1.456	0.7278	0.23	0.80187
	Vc×F	4	2.23%	7.656	1.9139	0.60	0.67529
	F×Af	4	3.88%	13.310	3.3274	1.05	0.45595
	Rbec×F	4	11.68%	40.075	10.0187	3.15	0.10154
	Error	6	5.55%	19.058	3.1764		
Dim.Dev	Rbec	2	9.00%	15.630	7.8148	2.93	0.12944
	Vc	2	56.36%	97.852	48.9259	18.35	0.00278
	F	2	12.07%	20.963	10.4815	3.93	0.08111
	Af	2	5.93%	10.296	5.1481	1.93	0.22526
	Vc×F	4	4.69%	8.148	2.0370	0.76	0.58532
	F×Af	4	1.37%	2.370	0.5926	0.22	0.91646
	Rbec×F	4	1.37%	2.370	0.5926	0.22	0.91646
	Error	6	9.22%	16.000	2.6667		
Geo.Dev	Rbec	2	41.99%	94.889	47.4444	12.94	0.00667
	Vc	2	0.88%	2.000	1.0000	0.27	0.77025
	F	2	28.61%	64.667	32.3333	8.82	0.01636
	Af	2	1.87%	4.222	2.1111	0.58	0.59055
	Vc×F	4	12.68%	28.667	7.1667	1.95	0.22082
	F×Af	4	0.79%	1.778	0.4444	0.12	0.96971
	Rbec×F	4	3.44%	7.778	1.9444	0.53	0.71926
	Error	6	9.73%	22.000	3.6667		
MRR	Rbec	2	0.00%	0.0001	0.00004	0.21	0.81304
	Vc	2	43.37%	14.7053	7.35266	40660.06	0.00000
	F	2	49.35%	16.7314	8.36570	46262.11	0.00000
	Af	2	0.04%	0.0127	0.00635	35.11	0.00049
	Vc×F	4	7.23%	2.4509	0.61272	3388.34	0.00000
	F×Af	4	0.01%	0.0021	0.00053	2.93	0.11615
	Rbec×F	4	0.00%	0.0010	0.00025	1.39	0.34078
	Error	6	0.00%	0.0011	0.00018		

The results indicate that two interactions have a statistically significant effect on responses. The *Rbec* × *F* interaction shows a significant influence on Ra, with a contribution of 13.75%, highlighting that the effect of feed rate depends on the tool nose radius. This reveals a nonlinear surface-generation mechanism in which tool geometry directly modulates the effect of feed rate on surface roughness. Likewise, the *Vc* × *F* interaction is significant for MRR, contributing 7.23%, which agrees with its analytical formulation showing a direct propor–tional relationship with both factors. All other inter–actions, including *F* × *Af* and *Vc* × *F* for the roughness and deviation responses, remain statistically non-signi–ficant. Their marginal contribution confirms that, for most outputs, the factors act essentially independently.

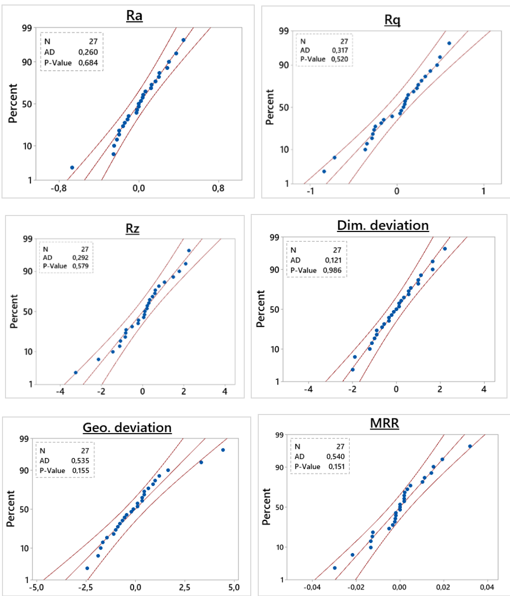

Figure 10. Normal probability plots -95% CI for responses

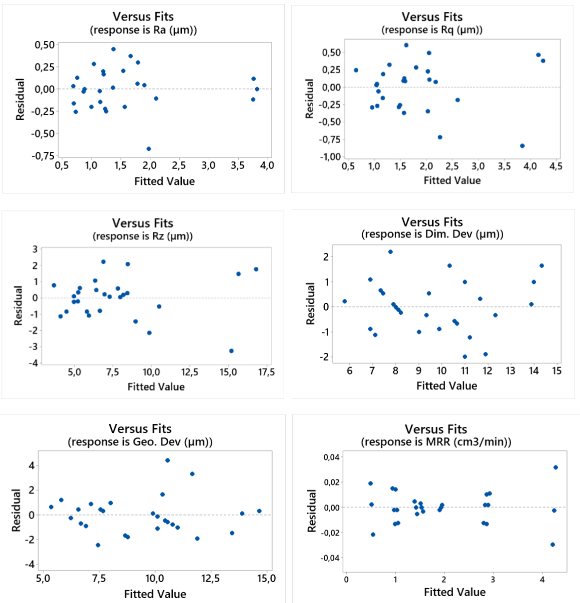

Figure 11. Versus fit plots for responses

3.3 Optimization using desirability approach

The reliability of the developed model to predict the target characteristics was previously demonstrated through Taguchi experiments, S/N ratio and ANOVA. However, when several responses are considered simul–taneously, especially when they exhibit conflicting trends, it becomes difficult to improve one output wit–hout degrading another. For instance, the minimization of the mean surface roughness Ra needs the selection of the lowest feed rate, which induces the lowest value of MRR that reduces significantly the productivity. Therefore, the objective is to find a balanced comp–romise among all performance indicators. In this context, multi-objective optimization proves particularly valuable for facilitating decision-making in complex situations. For the current study, the desirability function approach (DF) is adopted, a well-established method in manufacturing process optimization has been widely used and has demonstrated its high effectiveness in various industrial applications. For example, in machining, by converting multiple responses into a single, efficiently optimizable composite index.

This method is based on a straightforward concept: if the response value falls outside pre-established levels of desirability, it will be considered unacceptable. Consequently, the goal is to discover the parameter combination that produces the most desirable value for every individual response. All response variables y_i are first transformed into a normalized scale within the interval [0,1], from which an individual desirability index *di* is computed, where *di* = 0 demonstrates the range of unacceptable response y_i, while *di* = 1 means the optimal objective of the individual output y_i is achieved. To minimize an individual response, the desirability is quantified using the Smaller-The-Better criterion, as expressed in Equation3. In contrast, for responses that must be maximized, such as MRR, the desirability is calculated using the Larger-The-Better criterion, as defined in Equation 4.

$$di = \begin{cases} 0 & y_i > U \\ \left(\dfrac{y_i - U}{L - U}\right)^r & L \le y_i \le U \\ 1 & y_i < L \end{cases} \quad (3)$$

$$di = \begin{cases} 0 & y_i < U \\ \left(\dfrac{y_i - U}{L - U}\right)^r & L \le y_i \le U \\ 1 & y_i > L \end{cases} \quad (4)$$

where *di* is the ith desirability value of each response, *r* is a user-defined parameter used to adjust the importance of the response, and *U* and *L* respectively, denote the upper and lower limits of the individual output function.

Optimal individual desirability corresponds to the configuration where desirability value tends towards the value 1. These indices of individual desirability will subsequently be combined into a weighted geometric mean to obtain a composite desirability index D expressed by equation 5. The optimal parameter set is assigned to the experimental or simulated configuration exhibiting the highest composite desirability value.

$$D = \left((d1)^{w1}(d2)^{w2}\dots(dn)^{wn}\right)^{1/\sum wi} \quad (5)$$

where n is the number of individual responses in DoE, and w_i is the user-specified weight assigned to the i^{th} desirability function.

Regarding study constraints and context, they are illustrated in Table 7. They represents to the dimen–sional and geometrical specifications as required for specimen machining in accordance with ASTM E466. The individual and composite desirability results are presented in Table 8.

Table 7. Optimal range of cutting parameters/responses

Condition	Goal	Lower value	Upper value
Cutting speed (m/min)	In range	17	47
Feed rate (mm/rev)	In range	0.05	0.15
Tool nose radius (mm)	In range (categorical)	0.2	0.8
Depth of cut (mm)	In range	0.25	0.75
Ra (µm)	Minimize	-	0.8
Rq (µm)	Minimize	-	-
Rz (µm)	Minimize	-	-
Geometric dev. (µm)	Minimize	-	20
Dimensional devi. (µm)	Minimize	-	20
MRR (cm3/min)	Maximize	-	-

The optimal ANOVA–DF configuration was obta–ined, yielding the optimal set of input parameters (*Rbec* = 0.8, *Vc* = 32, *F* = 0.05, *Af* = 0.05), along with the corresponding predicted output responses. This configuration is subsequently validated experimentally and compared with the corresponding predicted ones as presented in Table 9. For surface roughness, the maxi–mum relative deviation remained below 5.5% for Ra and Rq, and below 10% for Rz. Dimensional and geo–metric deviations were also consistent with the predic–tions, with mean relative errors of 6.94% and 5.56%, respectively. The MRR showed a low error of 0.1%, further confirming the robustness of the approach. Alt–hough Rz exhibited slightly higher errors than the other roughness metrics, these remained acceptable at below 10%. Overall, the model demonstrates strong capability to capture the cutting responses of Ti-6Al-4V turned components. The Rz response showed high deviation, which can be attributed to local alterations to the mac–hined surface, such as burrs, built-up edges or vibration marks. This was further investigated using optical microscopy surface analysis, which revealed the presence of these irregularities as depicted in Figure 12 and Figure 13. Since Rz represents the maximum peak-to-valley height, it is more sensitive to localised surface defects, this makes predicting particularly challenging.

A comparison between the experimental results of the optimal configuration obtained using ANOVA–DF approach and the best setting from the DoE L27 (Run N19) Taguchi design, as reported in Table 10, reveals a significant enhancement of quality-related responses. Reductions of 22.8% in Ra, 21.4% in Rq, and 13.3% in Rz are achieved, along with improvements in dimen–sional and geometric of 20% and 16.7%, respectively. A marginal decrease in MRR (1.3%) is observed, which remains an acceptable trade-off for improved surface integrity and tolerance control in Ti-6Al-4V machining.

Table 8. Desirability and composite desirability of cutting responses

Run N	Response desirability						Composite desirability	
	Ra	Rq	Rz	Dim. dev	Geo. dev	MRR	Value	Rank
1	0.000	0.761	0.750	0.889	0.756	0.009	0.000	-
2	0.000	0.656	0.680	0.856	0.744	0.137	0.000	-
3	0.000	0.119	0.188	0.567	0.400	0.265	0.000	-
4	0.000	0.791	0.765	1.000	0.878	0.121	0.000	
5	0.000	0.650	0.648	0.811	0.700	0.368	0.000	-
6	0.000	0.196	0.216	0.778	0.422	0.635	0.000	-
7	0.000	0.655	0.617	0.433	0.733	0.233	0.000	-
8	0.000	0.596	0.559	0.478	0.622	0.620	0.000	-
9	0.000	0.096	0.114	0.367	0.444	0.985	0.000	-
10	0.000	0.843	0.784	0.533	0.844	0.246	0.000	-
11	0.000	0.773	0.745	0.500	0.833	0.611	0.000	-
12	0.000	0.512	0.517	0.211	0.489	0.977	0.000	-
13	0.167	0.902	0.904	0.911	0.967	0.001	0.230	3
14	0.000	0.796	0.819	0.700	0.789	0.129	0.000	-
15	0.000	0.618	0.651	0.667	0.511	0.278	0.000	-
16	0.000	0.896	0.873	0.867	0.922	0.113	0.000	-
17	0.000	0.873	0.847	0.911	0.811	0.381	0.000	-
18	0.000	0.648	0.666	0.800	0.633	0.627	0.000	-
19	**0.279**	**1.000**	**0.956**	**0.822**	**0.467**	**0.128**	**0.485**	**1**
20	0.000	0.906	0.872	0.789	0.456	0.374	0.000	-
21	0.000	0.766	0.779	0.500	0.111	0.621	0.000	-
22	0.112	0.904	0.854	0.411	0.489	0.240	0.401	2
23	0.000	0.769	0.723	0.200	0.311	0.605	0.000	-
24	0.000	0.712	0.690	0.167	0.033	0.992	0.000	-
25	0.253	0.927	0.928	0.611	0.444	0.000	0.000	-
26	0.000	0.875	0.857	0.656	0.333	0.144	0.000	-
27	0.000	0.771	0.810	0.544	0.156	0.271	0.000	-

Table 9. **ANOVA-DF predicted values and experimental validation for optimal parameters**

Response	Optimal parameters	Predicted value	Experimental value	Error (%)
Ra	Rbec = 0.8 Vc = 32 F = 0.05 Af = 0.5	0.568	0.558	1.78
Rq		0.664	0.703	5.52
Rz		3.48	3.86	9.84
Dim.Dev		7.444	8.00	6.94
Geo.Dev		9.444	10.00	5.56
MRR		0.964	0.964	0.1

Table 10. Experimental results comparison between ANOVA–DF optimum and L27 (Run N19) Taguchi design

Configuration	Input parameters				Responses					
	Rbec	Vc	F	Af	Ra	Rq	Rz	Dim.Dev	Geo.Dev	MRR
Optimal Taguchi L27 (Run N19) Exp.	0,8	32	0.05	0.25	0.723	0.894	4.454	10	12	0.977
Optimal ANOVA-DF Exp.	0.8	32	0.05	0.5	0.558	0.703	3.86	8	10	0.964
	Improvement (%)				+22.8	+21.4	+13.3	+20	+16.7	-1.3

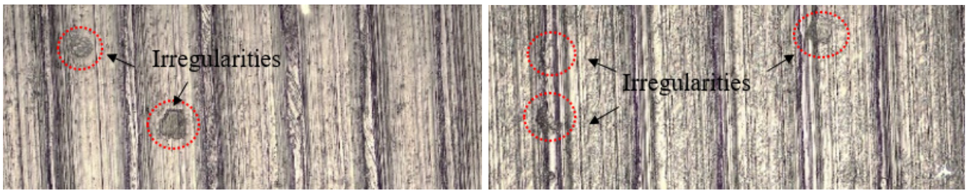

Figure 12. Machined surface texture observed by optical microscope Eclipse LV150N Nikon at X10 magnification

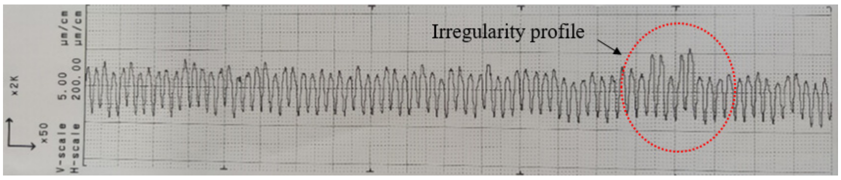

Figure 13. Surface roughness profile under *Vc* 17 m/min, *F* 0.05 mm/rev, *Af* 0.25 mm and *Rbec* 0.2

3.4 Artificial neural network prediction

Neural Network toolbox implemented in MATLAB 2024a was used to create a predictive model to capture the machining process. The input layer contain four neurons representing the machining parameters (*Rbec*, *Vc, F* and *Af*), while the output layer had six neurons that corresponded to the target responses defined (Ra, Rq, Rz, Dim.Dev, Geo.Dev and MRR). Selecting an appropriate network architecture is essential to avoid two major issues: overfitting, which occurs when there are too many hidden layers or neurons, causes the model to memorise experimental noise rather than capture the underlying physical behaviour, and under-fitting, which arises when the network is too simple to represent the inherent non-linearity of the machining responses.

Three learning algorithms, available in the MATLAB environment [58,59], are used in this study: Levenberg-Marquardt (LM), Bayesian Regularization (BR), and Sca–led Conjugate Gradient (SCG). The LM algorithm provi–des extremely fast convergence for medium-sized prob–lems [60]. The BR algorithm adds a new type of regula–rization by combining the sum of squared errors with the sum of squared weights [61]. The SCG is an efficient opti–mization algorithm that reduces memory requirements while maintaining numerically stability [62]. The proposed neural network architecture is presented in Figure 14 (a) and (b).

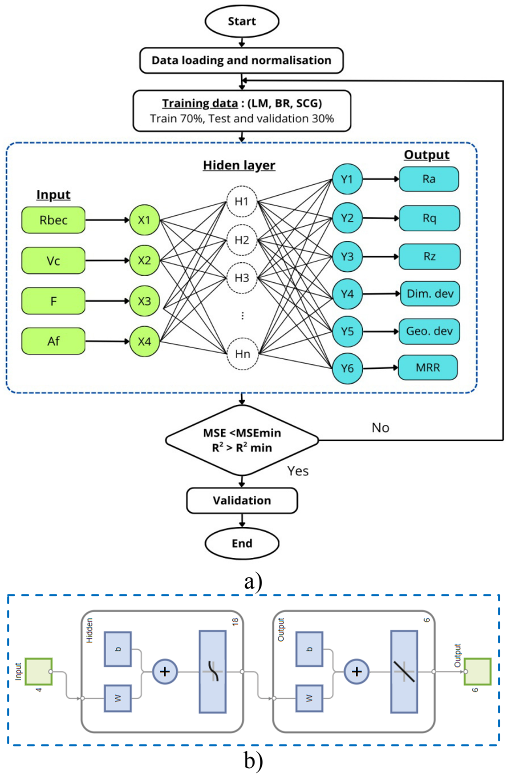

Figure 14. Neural Network Fetting in Matlab Toolbox: a) ANN algorithms model, b) ANN architecture

The actual dataset, including the selected input parameters and the corresponding output responses, was normalized to the [0,1] interval. To assess model robustness, a multi-run training protocol was employed, whereby each combination of learning algorithm was repeated. For each configuration, a new network was initialised, and the dataset was randomly partitioned into train (70%), validation (15%), and test (15%). The model performance was evaluated using statistical metrics, including the mean squared error (MSE) expressed by Equation 6, and the coefficient of determination (R^2) expressed by Equation 7. The best-performing configuration was selected in order to minimise MSE while prioritizing solutions with an R^2 value close to 1.

$$MSE = \frac{1}{n}\sum_{i=1}^{n}\left(y_i - \hat{y}i\right)^2 \tag{6}$$

$$R^2 = 1 - \frac{\sum_{i=1}^{n}\left(y_i - \hat{y}i\right)^2}{\sum_{i=1}^{n}\left(y_i - \bar{y}i\right)^2} \tag{7}$$

where n is the number of dataset, y_i is the i^{th} actual (Taguchi L27) data point value, $\hat{y}_i$ is the i^{th} predicted data point value, and □ is the mean of the actual output values. Lower MSE values (closer to zero) indicate better predictive accuracy. The coefficient of determination R^2 quantifies the proportion of variance in the experimental data, values approaching to 1 indicate an excellent fit.

The adopted approach involves iterative exploration of ANN architectures by varying the number of hidden layers and neurons per layer. Due to the limited dataset size, the search is restricted to a maximum of three hidden layers, each containing 5 to 20 neurons. This range, based on empirical recommendations (lower, middle, and upper bounds) to address adequate coverage while controlling model complexity and mitigating overfitting. A repeated training scenario in order of 1000 iterations is conducted to assess model robustness and stability.

BR algorithm with a single hidden layer of 18 neurons achieved the highest predictive performance as shown in Figure 15 and Figure 16, with the best correlation metrics as listed in Table 11. These findings demonstrate that a compact single hidden layer architecture is sufficient to capture the relationships between input parameters and machining responses, providing an optimal balance between accuracy, robustness, and simplicity. All responses exhibit excellent predictive capability.

Table 11. Performance metrics of optimised ANN architecture

Responce	MSE	R2
Ra	0.00788	0.9904
Rq	0.00049	0.99949
Rz	0.08116	0.99361
Dim.Dev	0.2993	0.95346
Geo.Dev	0.06401	0.99235
MRR	0.00973	0.99225

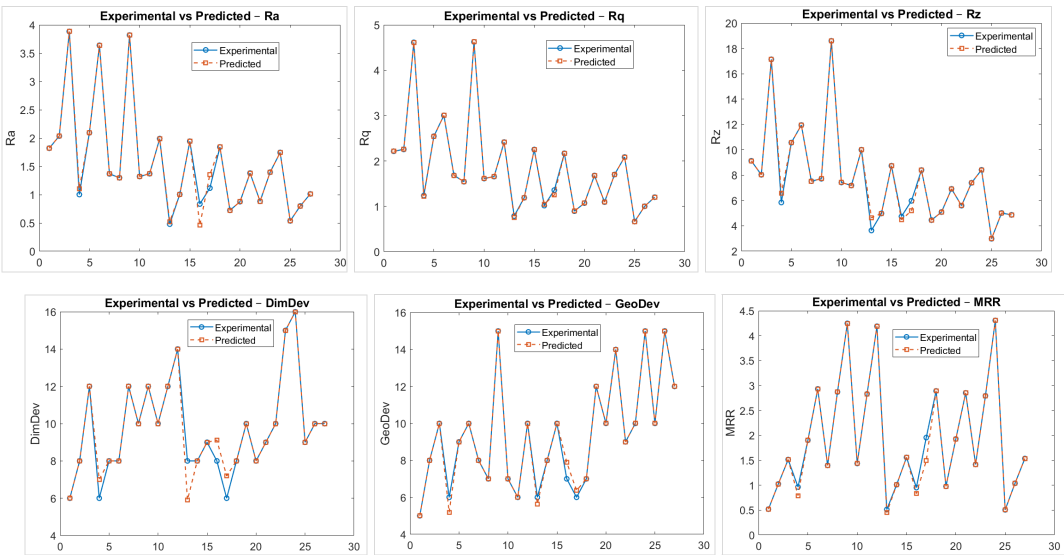

Figure 15. Actual (experimental) vs predicted responses

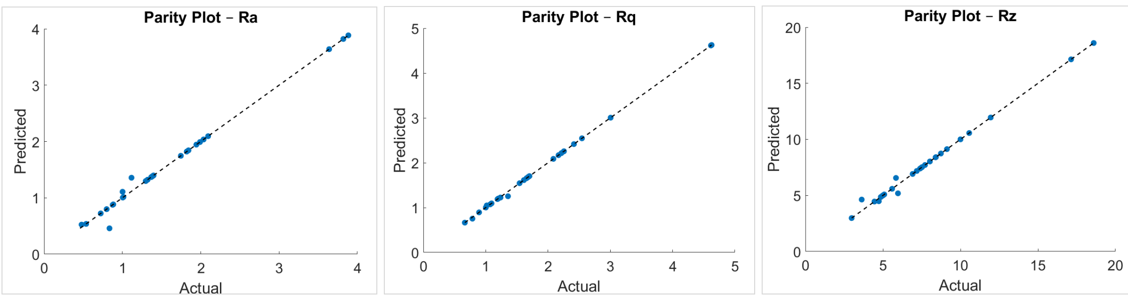

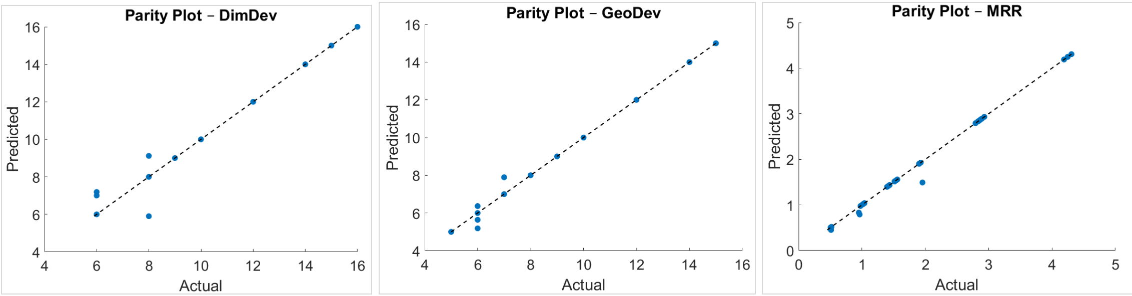

Figure 16. Parity plots Predicted vs actual values

3.5 Genetic Algorithm optimisation

In this section, a multi-objective optimisation strategy is adopted, combining ANN predictive capability with GA efficiency. Trained and validated on the experimental dataset, the ANN serves as a reliable surrogate model, enabling rapid and accurate estimation of the machining responses for candidate set of input parameters. To address the conflicting objectives of minimising surface roughness and dimensional/geometrical deviations while simultaneously maximising productivity linked to MRR, the optimisation framework is based on a weigh–ted desirability function approach.

As mentioned before in Table 7, A set of strict constraints is imposed, Ra ≤ 0.8 µm, DimDev ≤ 0.02 mm, and GeoDev ≤ 0.02 mm. These constraints are defined based on the dimensional and geometrical re–quirements for specimen machining according to ASTM E466. Any violation of these limits results in the addition of a severe penalty term to the fitness function, ensuring that infea–sible solutions are systematically excluded by the GA.

Table 12 . GA Parameters

Population Size	Max Generations	Max Stall Generations	Function Tolerance
300	400	200	1×10□□

The GA Parameters are illustrated in Table 12 [63–66]. For the purpose of ensuring sufficient genetic di–versity for adequate reliable global search of the highly nonlinear ANN-based surrogate landscape, a population of 300 individuals was chosen. To achieve a practical balance between reliably converging to a solution while also keeping the overall computational expense relatively low, a maximum generation limit of 400 was established and the stall condition of 200 generations. For the composite desirability index to be successfully maximised accurately, a maximum function tolerance of $1x10^{-8}$ was implemented. Restrictions on Ra, Dim.Dev and Geo.Dev were applied, and a snapping procedure was adopted to deal with the discrete requirement of tool nose radius. All the above settings were designed to help ensure that stable convergence would continue to lead towards optimal combinations of machining parameters, while also being compliant with a very strict level of quality requirements.

The weighted desirability GA, successfully used to determine an optimal machining compromise that simultaneously satisfies surface roughness, geometric/ dimensional accuracy, and productivity requirements for Ti-6Al-4V machining. As presented in Table 13, the results meets the key constraint Ra < 0.8 µm (achieving Ra = 0.33 µm), while keeping both dimensional and geometric deviations well below 20 µm (6.5 to 6.8 µm). The level of productivity at MRR=0.914 cm3/min shows that the improved surface quality was not obta–ined by significantly compromising the rate of material removal. The optimum parameters founded are *Rbec* = 0.4 mm, *Vc* ≈ 25 m/min, *F* = 0.065 mm/rev, *Af* ≈ 0.7 mm, corresponds to a low feed rate and a relatively sharp cutting edge, consistent with the physical mecha–nisms improving surface roughness.

The GA-derived optimum was experimentally validated to provide an accurate and reliable evaluation of the predictive framework in order to validate the global optimization approach. In general, the results of the experiment supported the agreement between the predicted values derived from the ANN–GA and the experimental measurements (Table 14). In terms of surface roughness (Ra, Rq, and Rz), the maximum deviation from the predicted values was consistently below 6%, which demonstrates that the predictive model is capable of capturing the surface integrity performance of Ti-6Al-4V turned parts. In addition, the dimensional and geometric parameters were also consistent with their corresponding predicted values, exhibiting an average relative error of only 4.84% for dimensional parameters and 2.86% for geometric parameters. Finally, MRR had a minimal deviation of only 0.1%, which also further supports the robustness and reliability of the predictive approach.

Table 13. ANN-GA optimal predicted input and output parameters

Optimal Input parameters				Optimal responses					
Rbec (mm)	Vc (m/min)	F (mm/rev)	Af (mm)	Ra (µm)	Rq (µm)	RZ (µm)	Dim. Dev (µm)	Geo. Dev (µm)	MRR (cm3/min)
0.4	25	0.065	0.7	0.33	0.59	3.10	6.5	6.8	0.914

Table 14. Comparison of optimal ANN-GA Predicted and experimental validation

Response	Optimal parameters	Predicted	Experimental	Error
Ra	Rbec = 0.4	0.33	0.34	2.94 %
Rq	Vc = 25	0.59	0.57	3.51 %
Rz	F = 0.065	3.10	2.94	5.44 %

Dim.Dev	Af = 0.7	6.5	6.2	4.84 %
Geo.Dev		6.8	7	2.86 %
MRR		0.914	0.914	0.01 %

Table 15. Comparison of optimal desirability composite configuration for ANOVA and GA approach

Configuration	Input parameters				Responses					
	Rbec	Vc	F	Af	Ra	Rq	Rz	Dim.Div	Geo.Div	MRR
Optimal ANOVA-DF Exp.	0.8	32	0.05	0.5	0.558	0.703	3.86	8	10	0.964
Optimal ANN-GA Exp.	0.4	25	0.065	0.7	0.34	0.57	2.94	6	7	0.913
	Improvement (%)				+39.07	+18.92	+23.83	+25	+30	-5.29

Compared with the ANOVA–DF approach, the ANN–GA hybrid offers a clear improvement in the quality of the machined specimens (Table 15). By selec–ting a better-balanced set of machining parameters, ANN–GA enhances several quality responses at the same time. Relative to the ANOVA optimum, it reduces Ra, Rq, and Rz by 39%, 19%, and 24%, respectively. Similar improvements are found for accuracy, with dimensional and geometric deviations decreasing by 25% and 30%, confirming its ability to capture the non-linear interac–tions inherent to the turning process. These results show that ANN–GA is more effective than the conventional statistical approach for handling complex multi-objective trade-offs. Even if the coupled approach induces a decrease of 5% in MRR, this remains acceptable when prioritizing surface finish and tighter tolerances.

4. CONCLUSION

To sum up, the current study dealt with the analysis and optimization of the machinability of Ti-6Al-4V titanium alloy. Cylindrical specimens were manufactured for fatigue testing, with tight geometric and dimensional specifications in accordance to ASTM E466. An experimental study was carried out to assess the influence of several cutting parameters, such as cutting speed, feed rate, depth of cut and tool radius on many responses. These were surface roughness, which en–compasses arithmetic mean roughness (Ra), root mean square roughness (Rq), and maximum peak-to-valley height (Rz), and their dimensional and geometric accuracy, and material remove rate. Two methods were adopted and compared for multi-objective optimization of turning process of Ti-6Al-4V alloy. The first method based on Taguchi design of experiments method coup–led with ANOVA and DF, while the second method used ANN coupled with a GA and DF. The significance of the input parameters and their interactions on cutting responses was determined by the first method. Then, DF was applied to perform multi-objective optimization. On the other hand, A hybrid ANN-GA framework was implemented to resolve the conflicts among the competing multi objectives optimisation, by DF. Accor–ding to experiments and result analysis, the next conclusions can be drawn:

- Based on Taguchi S/N ratio analysis, the surface roughness is strongly affected by *F* and Rbec. Dimensional deviation is mainly governed by *Vc*. Geometric deviation is strongly influenced by *Rbec*, while MRR is governed by *Vc* and *F*.
- The Taguchi and ANOVA results showed that the most significant interactions, along with their contributions, are *Rbec* × *F* for Ra (13.75%) and *Vc* × *F* for MRR (7.23%).
- The ANOVA results revealed that *F* is the most dominant factor affecting surface roughness, cont–ributing 41.1% to Ra and 38.56% to Rq, while *Rbec* accounts for 37.1% to Rz. For dimensional devi–ation, *Vc* is the primary influencing parameter, with a contribution of 56.36%, whereas *Rbec* contributes 41.99% to geometric deviation. Regarding MRR, *Vc* has the strongest effect of 49.35%, followed by *F* of 43.37%.
- A coupled ANOVA-DF was performed to resolve conflicts among the competing objectives aim is to minimise surface roughness, dimensional and geo–metric deviations while maximise MRR. Optimal configuration set *Rbec* 0.8 mm, *Vc* 32 m/min, *F* 0.05 mm, *Af* 0.5 mm. comparable to the Taguchi optimal configuration, ANOVA-DF results achie–ves improvement of 23 % in Ra, 21.4% in Rq, and 13.3% in Rz, 20% in Dim.Dev, et 17% in Geo.Dev, minor reduction in MRR (1.3%).
- A hybrid ANN-GA was implemented to predict and optimise the studied responses, based on DF the optimal set parameters (*Rbec* = 0.4 mm, *Vc* = 25 m/min, *F* = 0.065 mm/rev, *Af* = 0.7 mm). Compared to ANOVA-DF, ANN-GA-DF demons–trating markedly superior performance, this model enabled a marked improvement in surface rough–ness (Ra 39%, Rq 19%, and Rz 24%), while simultaneously enhancing dimensional and geom–etric accuracy by 25% and 39%, at a limited reduc–tion in cost productivity in MRR of 5.3%.
- This study highlights the strong potential of hybrid data-driven strategies for optimizing complex manufacturing processes. However, the application of guidelines and recommendations derived from experimental and AI-based results should be care–fully evaluated, and their scope of application clearly defined. This represents a promising direc–tion for future research. Future work could extend the proposed hybrid data-driven strategy toward real-time adaptive optimization of Ti-6Al-4V machining. This requires integrating sensor-based data, such as cutting forces, temperature, vibration, and tool wear. Further studies should also assess the robustness of the models under various cutting conditions, tool geometries, and machining envi–ronments. In addition, the framework could be

expanded by considering other responses, namely tool wear, residual stresses, energy consumption, and machining cost, to better address quality, productivity, and sustainability requirements. Finally, this approach could be applied to other difficult-to-cut materials and extended to other machining processes. It could also be integrated into digital twin-based intelligent manufacturing systems.

REFERENCES

[1] Yin, J., Sun, R., Ming, C., Chen, C., Zeng, S.: Investigation of Single Grain Grinding of Titanium Alloy Using Diamond Abrasive Grain with Positive Rake Angle. Machines, Vol. 12, paper 451, 2024.

[2] Cui, C., Hu, B., Zhao, L., Liu, S.: Titanium alloy production technology, market prospects and ind–ustry development. Materials & Design, Vol. 32, No. 3, pp. 1684–1691, 2011.

[3] Arrazola, P.-J., Garay, A., Iriarte, L.-M., Armendia, M., Marya, S., Le Maître, F.: Machinability of titanium alloys (Ti6Al4V and Ti555.3). Journal of Materials Processing Technology, Vol. 209, No. 5, pp. 2223–2230, 2009.

[4] Gupta, K., Laubscher, R. F.: Sustainable machining of titanium alloys: A critical review. Proceedings of the Institution of Mechanical Engineers, Part B: Journal of Engineering Manufacture, Vol. 231, No. 14, pp. 2543–2560, 2017.

[5] López De Lacalle, L. N., Pérez, J., Llorente, J. I., Sánchez, J. A.: Advanced cutting conditions for the milling of aeronautical alloys. Journal of Materials Processing Technology, Vol. 100, No. 1-3, pp 1–11, 2000.

[6] Le Coz, G., Marinescu, M., Devillez, A., Dud–zinski, D., Velnom, L.: Measuring temperature of rotating cutting tools: Application to MQL drilling and dry milling of aerospace alloys. Applied Thermal Engineering, Vol. 36, pp. 434–441, 2012.

[7] Revuru, R. S., Posinasetti, N. R., Vsn, V. R., M, A.: Application of cutting fluids in machining of titanium alloys—a review. The International Jour–nal of Advanced Manufacturing Technology, Vol. 91, No. 5-8, pp. 2477–2498, 2017.

[8] Molinari, A., Musquar, C., Sutter, G.: Adiabatic shear banding in high speed machining of Ti–6Al–4V: experiments and modeling. International Jour–nal of Plasticity, Vol. 18, No. 4, pp. 443–459, 2002.

[9] Che-Haron, C. H., Jawaid, A.: The effect of mac–hining on surface integrity of titanium alloy Ti–6% Al–4% V. Journal of Materials Processing Tech–nology, Vol. 166, No. 2, pp. 188–192, 2005.

[10] Lee, W.-S., Lin, C.-F.: High-temperature deforma–tion behaviour of Ti6Al4V alloy evaluated by high strain-rate compression tests. Journal of Materials Processing Technology, Vol. 75, No. 1-3, pp. 127–136, 1998.

[11] Sun, S., Brandt, M., Dargusch, M. S.: Characte–ristics of cutting forces and chip formation in machining of titanium alloys. International Journal of Machine Tools and Manufacture, Vol. 49, No. 7-8, pp. 561–568, 2009.

[12] Barry, J., Byrne, G., Lennon, D.: Observations on chip formation and acoustic emission in machining Ti–6Al–4V alloy. International Journal of Machine Tools and Manufacture, Vol. 41, No. 7, pp 1055–1070, 2001.

[13] Chen, X., Tang, J., Ding, H., Liu, A.: Experimental study on the evolution of chip morphology, chip formation, and surface topography with cutting parameters, and their relationships in dry milling of cast aluminum alloy with PCD inserter. Journal of Mechanical Science and Technology, Vol. 35, No. 4, pp. 1651–1662, 2021.

[14] Zhang, X., Zhang, J., Pang, B., Zhao, W.: An accu–rate prediction method of cutting forces in 5-axis flank milling of sculptured surface. International Journal of Machine Tools and Manufacture, Vol. 104, pp. 26–36, 2016.

[15] Sun, S., Brandt, M., Dargusch, M. S.: Charac–teristics of cutting forces and chip formation in machining of titanium alloys. International Journal of Machine Tools and Manufacture, Vol. 49, No. 7-8, pp. 561–568, 2009.

[16] Mabrouki, T., Rigal, J.-F.: A contribution to a qua–litative understanding of thermo-mechanical effects during chip formation in hard turning. Journal of Materials Processing Technology, Vol. 176, No. 1-3, pp. 214–221, 2006.

[17] Chtioui, A., Ouballouch, A., Mouchtachi, A.: In–vestigation of Cutting Responses During High-speed Machining of Ti6Al4V Alloy: Finite Element Analysis. FME Transactions, Vol. 52, No. 4, pp. 616–627, 2024.

[18] Ulutan, D., Ozel, T.: Machining induced surface integrity in titanium and nickel alloys: A review. International Journal of Machine Tools and Manu–facture, Vol. 51, No. 3, pp. 250–280, 2011.

[19] Motorcu, A., Ekici, E.: Evaluation and multi-cri–teria optimization of surface roughness, deviation from dimensional accuracy and roundness error in drilling CFRP/Ti6Al4 stacks. FME Transactions, Vol. 50, No. 3, pp. 441–460, 2022.

[20] Wang, Z.-M., Jia, Y.-F., Zhang, X.-C., Fu, Y., Zhang, C.-C., Tu, S.-T.: Effects of Different Mec–hanical Surface Enhancement Techniques on Sur–face Integrity and Fatigue Properties of Ti-6Al-4V: A Review. Critical Reviews in Solid State and Materials Sciences, Vol. 44, No. 6, pp. 445–469, 2019.

[21] Javidi, A., Rieger, U., Eichlseder, W.: The effect of machining on the surface integrity and fatigue life. International Journal of Fatigue, Vol. 30, No. 10-11, pp. 2050–2055, 2008.

[22] Khan, A. M., He, N., Li, L., Zhao, W., Jamil, M.: Analysis of Productivity and Machining Efficiency in Sustainable Machining of Titanium Alloy. *Procedia Manufacturing*, Vol. 43, pp. 111–118, 2020.

[23] Shaw, M. C.: *Metal cutting principles*, Ed., Oxford series on advanced manufacturing, 2nd ed., Oxford University Press, New York, 2005.

[24] Khan, A. M., Jamil, M., Salonitis, K., Sarfraz, S., Zhao, W., He, N., Mia, M., Zhao, G.: Multi-Objec–tive Optimization of Energy Consumption and Surface Quality in Nanofluid SQCL Assisted Face Milling. Energies, Vol. 12, No. 4, pp. 710, 2019.

[25] Gupta, M. K., Mia, M., Jamil, M., Singh, R., Singla, A. K., Song, Q., Liu, Z., Khan, A. M., Rahman, M. A., Sarikaya, M.: Machinability inves–tigations of hardened steel with biodegradable oil-based MQL spray system. The International Journal of Advanced Manufacturing Technology, Vol. 108, No. 3, pp. 735–748, 2020.

[26] Kumar, R., Bilga, P. S., Singh, S.: Multi objective optimization using different methods of assigning weights to energy consumption responses, surface roughness and material removal rate during rough turning operation. Journal of Cleaner Production, Vol. 164, pp. 45–57, 2017.

[27] Ribeiro, M. V., Moreira, M. R. V., Ferreira, J. R.: Optimization of titanium alloy (6Al–4V) machi–ning. Journal of Materials Processing Technology, Vol. 143–144, pp. 458–463, 2003.

[28] Puertas Arbizu, I., Luis Pérez, C. J.: Surface rough–ness prediction by factorial design of experiments in turning processes. Journal of Materials Proces–sing Technology, Vol. 143–144, pp. 390–396, 2003.

[29] Sellappan, S. N., Chinnappandi, M., Jeyaraj, P. K., Seethalakshmi, S. K. S. P., Sulaiman, Z., Rahim Sulaiman, A. R. A.: Multi-Objective Optimization of Micromachining Parameters for Titanium Alloy Ti-3Al-2.5V Using Grey Relational Analysis. *In The 7th International Global Conference Series on ICT Integration in Technical Education & Smart Society, MDPI,* 03-09-2025, paper 51.

[30] Eltaggaz, A., Nouzil, I., Deiab, I.: Machining Ti-6Al-4V Alloy Using Nano-Cutting Fluids: Investi–gation and Analysis. Journal of Manufacturing and Materials Processing, Vol. 5, No. 2, paper 42, 2021.

[31] Tauviqirrahman, M., At Thariq, M. R., Puspitasari, P., Setiawan, A., Andoko, A., Pramono, D. D.: En–hanced Tribological Performance of Nano-Cutting Fluids with Soybean Oil and Hybrid h-BN/ MWCNT Additive Nanoparticles Utilizing the Mi–nimum Quantity Lubrication Method. FME Tran–sactions, Vol. 54, No. 2, pp. 369–379, 2026.

[32] Sztankovics, I., Rodić, D.: Comparative study of rotational and longitudinal turning: Energy effici–ency and surface roughness in machining norma–lized medium-carbon steel. FME Transactions, Vol. 54, No. 1, pp. 39–52, 2026.

[33] Yan, J., Li, L.: Multi-objective optimization of milling parameters – the trade-offs between energy, production rate and cutting quality. Journal of Cleaner Production, Vol. 52, pp. 462–471, 2013.

[34] Ramesh, S., Karunamoorthy, L., Palanikumar, K.: Measurement and analysis of surface roughness in turning of aerospace titanium alloy (gr5). Measurement, Vol. 45, No. 5, pp 1266–1276, 2012.

[35] Rahman, A. M., Rob, S. M. A., Srivastava, A. K.: Modeling and optimization of process parameters in face milling of Ti6Al4V alloy using Taguchi and grey relational analysis in, *Procedia Manufac–turing*, 06-2021, Ohio, USA, Vol. 53, pp. 204–212.

[36] Cica, D., Tesic, S., Markovic, M., Sredanovic, B., Borojevic, S., Zeljkovic, M., Kramar, D., Pušavec, F.: Multi-Objective Optimization of Milling Ti-6Al-4V Alloy for Improved Surface Integrity and Sustainability Performance. Machines, Vol. 13, No. 3, paper 221, 2025.

[37] Jamil, M., Khan, A. M., Hegab, H., Gupta, M. K., Mia, M., He, N., Zhao, G., Song, Q., Liu, Z.: Milling of Ti–6Al–4V under hybrid Al2O3-MWCNT nanofluids considering energy consump–tion, surface quality, and tool wear: a sustainable machining. The International Journal of Advanced Manufacturing Technology, Vol. 107, No. 9-10, pp. 4141–4157, 2020.

[38] Khan, M. A., Jaffery, S. H. I., Khan, M., Younas, M., Butt, S. I., Ahmad, R., Warsi, S. S.: Multi-objective optimization of turning titanium-based alloy Ti-6Al-4V under dry, wet, and cryogenic conditions using gray relational analysis (GRA). The International Journal of Advanced Manufac–turing Technology, Vol. 106, No. 9-10, pp. 3897–3911, 2020.

[39] Senthil Kumar L, Manivel C, Savadamuthu L: Multiobjective optimization process of Ti6Al4V alloy using MWCNTs dispersed cutting fluid in turning operation. Journal of Ceramic Processing Research, Vol. 23, No. 4, pp. 476–489, 2022.

[40] Younas, M., Jaffery, S. H. I., Khan, M., Khan, M A., Ahmad, R., Mubashar, A., Ali, L.: Multi-objec–tive optimization for sustainable turning Ti6Al4V alloy using grey relational analysis (GRA) based on analytic hierarchy process (AHP). The International Journal of Advanced Manufacturing Technology, Vol. 105, No. 1-4, pp. 1175–1188, 2019.

[41] Hossain, S., Abedin, M. Z., Saha, R. K., Touhi–duzzaman, M., Hossen, M. J.: RETRACTED: Op–timization of cutting temperature and surface roughness in CNC turning of Ti-6Al-4V alloy using response surface methodology. Heliyon, Vol. 11, No. 1, paper e41051, 2025.

[42] Özel, T., Karpat, Y.: Predictive modeling of surface roughness and tool wear in hard turning using regression and neural networks. International Journal of Machine Tools and Manufacture, Vol. 45, No. 4-5, pp. 467–479, 2005.

[43] Adizue, U. L. et al.: Surface quality prediction by machine learning methods and process parameter optimization in ultra-precision machining of AISI D2 using CBN tool. The International Journal of Advanced Manufacturing Technology, Vol. 129, No. 3-4, pp. 1375–1394, 2023.

[44] Bañon, F., Martin, S., Vazquez-Martinez, J. M., Salguero, J., Trujillo, F. J.: Predictive models based

on RSM and ANN for roughness and wettability achieved by laser texturing of S275 carbon steel alloy. Optics & Laser Technology, Vol. 168, paper 109963, 2024.

[45] Upadhyay, V., Jain, P. K., Mehta, N. K.: In-process prediction of surface roughness in turning of Ti–6Al–4V alloy using cutting parameters and vibration signals. Measurement, Vol. 46, No. 1, pp 154–160, 2013.

[46] Kim, B., Bae, J., Han, S. S.: Prediction of radio fre–quency power effect on silicon nitride deposition using a genetic algorithm based neural network. Surface Engineering, Vol. 22, No. 1, pp. 63–68, 2006.

[47] Bien, D. X.: Predictive modeling of surface rough–ness in hard turning with rotary cutting tool based on multiple regression analysis, artificial neural network, and genetic programing methods. Procee–dings of the Institution of Mechanical Engineers, Part B: Journal of Engineering Manufacture, Vol. 238, No. 1-2, pp. 137–150, 2024.

[48] Tian, W., Wang, W., Wang, Y., Zhang, S.: Study on Multi-Objective Optimization of Milling Process of Powder Metallurgy Titanium Aluminum Alloys. Manufacturing Technology, Vol. 24, No. 4, pp. 652–667, 2024.

[49] Milosevic, A., Ivanov, V., Simunovic, S., Vukelic, D.: Optimization of Grinding and Wheel Para–meters during External Cylindrical Longitudinal Machining of AISI 6150 Alloy Steel Based on Accuracy, Quality and Productivity. FME Tran–sactions, Vol. 54, No. 2, pp. 199–213, 2026.

[50] Li, J., Yang, X., Ren, C., Chen, G., Wang, Y.: Mul–tiobjective optimization of cutting parameters in Ti-6Al-4V milling process using nondominated sorting genetic algorithm-II. The International Journal of Advanced Manufacturing Technology, Vol. 76, No. 5-8, pp. 941–953, 2015.

[51] Escamilla-Salazar, I. G., Torres-Treviño, L. M., González-Ortíz, B., Zambrano, P. C.: Machining optimization using swarm intelligence in titanium (6Al 4V) alloy. The International Journal of Advanced Manufacturing Technology, Vol. 67, No. 1-4, pp. 535–544, 2013.

[52] Mane, S., Patil, R. B., Al-Dahidi, S.: Predictive Modeling of Surface Roughness and Cutting Tem–perature Using Response Surface Methodology and Artificial Neural Network in Hard Turning of AISI 52100 Steel with Minimal Cutting Fluid Appli–cation. Machines, Vol. 13, No. 4, paper 266, 2025.

[53] Elsadek, A. A., Gaafer, A. M., Mohamed, S. S., Mohamed, A. A.: Prediction and optimization of cutting temperature on hard-turning of AISI H13 hot work steel. SN Applied Sciences, Vol. 2, No. 4, paper 540, 2020.

[54] Mia, M., Khan, M. A., Dhar, N. R.: Study of sur–face roughness and cutting forces using ANN, RSM, and ANOVA in turning of Ti-6Al-4V under cryogenic jets applied at flank and rake faces of coated WC tool. The International Journal of Advanced Manufacturing Technology, Vol. 93, No. 1-4, pp. 975–991, 2017.

[55] Mia, M., Dhar, N. R.: Prediction of surface rough–ness in hard turning under high pressure coolant using Artificial Neural Network. Measurement, Vol. 92, pp. 464–474, 2016.

[56] Yan, J., Li, L.: Multi-objective optimization of mil–ling parameters – the trade-offs between energy, production rate and cutting quality. Journal of Cleaner Production, Vol. 52, pp. 462–471, 2013.

[57] Aswathy, V. G., Joseph, J., Pradeepmon, T. G., Sravan Kumar, A., Babu, A.: Multi-objective Opti–mization of Machining Parameters for Ti-6Al-4V Turning Using Genetic Algorithm, in: *Recent Advances in Logistics, Supply Chain and Transportation*, Vol. 1, 2026, pp. 123–130.

[58] Ciaburro, G.: *MATLAB for machine learning*: *un–lock the power of deep learning for swift and en–hanced results*, 2nd edition, packt, Birmingham, 2024.

[59] El Ghadoui, M., Mouchtachi, A., Majdoul, R.: A hybrid optimization approach for intelligent manu–facturing in plastic injection molding by using arti–ficial neural network and genetic algorithm. Scien–tific Reports, Vol. 13, No. 1, paper 21817, 2023.

[60] Hagan, M. T., Menhaj, M. B.: Training feedforward networks with the Marquardt algorithm. IEEE Transactions on Neural Networks, Vol. 5, No. 6, pp. 989–993, 1994.

[61] Dan Foresee, F., Hagan, M. T.: Gauss-Newton app–roximation to Bayesian learning, in: *Proceedings of International Conference on Neural Networks (ICNN'97)*, IEEE, Houston, TX, USA, 1997, Vol. 3, pp. 1930–1935.

[62] Meiller, M. F.: A Scaled Conjugate Gradient Algo–rithm for Fast Supervised Learning, neural networks, Vol. 6, pp. 523-533, 1993.

[63] García-Martínez, C., Rodriguez, F. J., Lozano, M.: Genetic Algorithms, in: *Handbook of Heuristics*; SN, Switzerland, Cham, pp. 627–662, 2025.

[64] Xingyi, Z.; Ran, C.; Ye, T.; Yaochu, J.: *Evolu–tionary Large-Scale Multi-Objective Optimization and Applications*, Wiley-IEEE Press, 2024.

[65] Akan, T., Anter, A. M., Etaner-Uyar, A. Ş., Oliva, D., Eds.: *Engineering Applications of Modern Metaheuristics*, SN Cham, ed. 1, 2023.

[66] Greiner, D., nio Gaspar-Cunha, A., Hern ́andez-Sosa, D., Minisci, E., Zamuda, A.: *Evolutionary Algorithms in Engineering Design Optimization*; MDPI, 2022.

NOMENCLATURE

Vc	cutting speed
F	feed rate
Af	depth of cut
Rbec	tool nose radius
di	desirability value
D	composite desirability
U	upper limit

L	low limit

Greek symbols

y_i	response value
$\bar{y}$	mean value
w_i	weight

Abreviations

Ra	arithmetic mean roughness
Rq	root mean square roughness
Rz	maximum peak-to-valley height
MRR	material removal rate
DF	desirability function
ANN	artificial neural networks
GA	genetic algorithms
NSGA	Non-Dominated Sorting GA
DoE	design of experiments
ANOVA	Analysis of variances
RSM	response surface methodology
AI	artificial intelligence
CNC	computer numerical control
CVD	chemical vapor deposition
S/N	signal-to-noise
Dim.Dev	dimensional deviation
Geo.Dev	geometric deviation
MSE	mean squared error
R^2	coefficient of determination

ВИШЕЦИЉНА ОПТИМИЗАЦИЈА СТРУГАЊА ЛЕГУРЕ ТИТАНИЈУМА Ti-6Al-4V КОРИШЋЕЊЕМ ДИЗАЈНА ЕКСПЕРИ– МЕНАТА, ВЕШТАЧКИХ НЕУРОНСКИХ МРЕЖА И ГЕНЕТСКИХ АЛГОРИТАМА

А. Чтиуи, А. Оубалоуш, А. Мухтачи

Овај рад представља експериментално истраживање обрадивости легуре титанијума Ti-6Al-4V. Фоку–сира се на утицај параметара резања на квалитет и продуктивност обрађених делова. За процену значаја параметара обраде и њихових интеракција користи се ортогонални низ Taguchi L27 у комбинацији са анализом варијансе. Вишециљна оптимизација заснована на функцији пожељности (DF) је извршена да би се одредили оптимални параметри резања. Штавише, хибридни модел вештачких неуронских мрежа-генетских алгоритама (ANN-GA) заснован на Taguchi L27 и повезан са DF је усвојен за предвиђање и оптимизацију одговора резања. ANN-GA-DF показује супериорне перформансе, постижући значајна побољшања у храпавости површине (39% у Ra, 19% у Rq, 24% у Rz), димензионалној и геометријској тачности (25% и 39%, респективно). Брзина уклањања материјала се благо смањује (5,3%). Оптимални параметри су полупречник алата од 0,4 мм, брзина резања од 25 м/мин, брзина помака од 0,065 мм/окретају и дубина резања од 0,7 мм.